Effects of Nanosecond Pulsed Electric Fields on the Intracellular Function of HeLa Cells As Revealed by NADH Autofluorescence Microscopy

Kamlesh Awasthi,[†] Takakazu Nakabayashi,[‡] and Nobuhiro Ohta*,[†]

[†]Department of Applied Chemistry and Institute of Molecular Science, National Chiao Tung University, 1001, Ta-Hsueh Road, Hsinchu 30010, Taiwan

[‡]Graduate School of Pharmaceutical Sciences, Tohoku University, 6-3 Aoba-ku, Sendai 980-8578, Japan

S Supporting Information

ABSTRACT: The fluorescence lifetime of the endogenous fluorophore of reduced nicotinamide adenine dinucleotide (NADH) in HeLa cells is affected by the application of nanosecond pulsed electric fields (nsPEFs). In this study, we found that after nsPEF application, the fluorescence lifetime became longer and then decreased in a stepwise manner upon further application, irrespective of the pulse width in the range of 10−50 ns. This application time dependence of the NADH fluorescence lifetime is very similar to the time-lapse dependence of the NADH fluorescence lifetime following the addition of an apoptosis inducer, staurosporine. These results, as well as the membrane swelling and blebbing after the application of nsPEFs, indicate that apoptosis is also induced by the application of nsPEFs in HeLa cells. In contrast to the lifetime, the fluorescence intensity remarkably depended on the pulse width of the applied nsPEF. When the pulse width was as large as 50 ns, the intensity monotonically increased and was distributed over the entire cell as the application duration became longer. As the pulse width of the applied electric field became smaller, the magnitude of the field-induced increase in NADH fluorescence intensity decreased; the intensity was reduced by the electric field when the pulse width was as small as 10 ns. These results suggest that the mechanism of electric-field-induced apoptosis depends on the pulse width of the applied nsPEF.
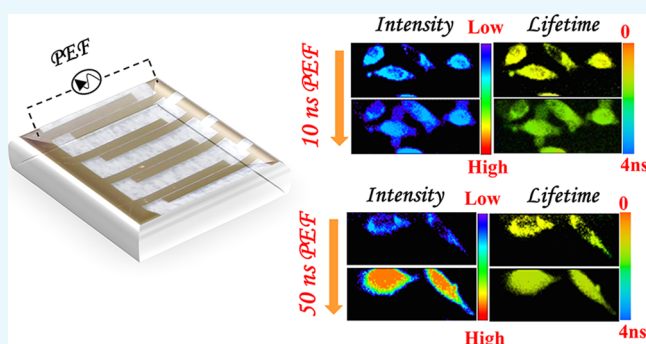
INTRODUCTION

Intracellular signaling plays a pivotal role in cell functioning, which requires coordinated and accurate transformation of information from organelles and/or signaling proteins to others through cell membranes. One of the best examples can be seen in programmed cell death, which is called apoptosis. During apoptosis, cells die in a highly coordinated manner, following the induction of the cell death signal. During the process, chromatin condensation and nucleus fragmentation occur without damage to the surrounding cells, which later induce structural changes, such as a reduction in cell volume and membrane blebbing. Mitochondria are well known as one of the key regulators of intracellular signaling in apoptosis. Many research groups have emphasized the role of certain biochemical processes, including the disruption of adenosine triphosphate (ATP) production through the alteration of electron transport processes, the alteration of cellular oxidation reduction, and the release of proteins that trigger the activation of caspase family proteases, which takes place in mitochondria during apoptosis.[1−6]

Several chemical substances trigger apoptosis, including death receptor-mediated apoptosis inducers such as staur-osporine (STS) and tumor necrosis factor (TNF)-α; however, it remains unclear why a variety of cells die in the same manner in response to the same substances and conditions.[7−10] A common feature of apoptosis is the transformation of both information and apoptotic-activated proteins from the inner membrane of mitochondria to other intracellular organelles due to the collapse of the transmembrane potential. This collapse opens voltage-dependent channels and results from the nonequilibrium of ions between the inner and outer spaces of mitochondria, which can be induced by apoptotic substances and death receptors.[11]

Over the past several years, significant progress has been made in delivering external biomolecules, DNA, and quantum dots into living cells and in intracellular recordings of the action potential through electroporation by pulsed electric fields (PEFs).[12−16] Along with this, a number of researchers have also reported electric-field-induced increases in intracellular calcium, nuclear perturbations, apoptosis, and other physiological
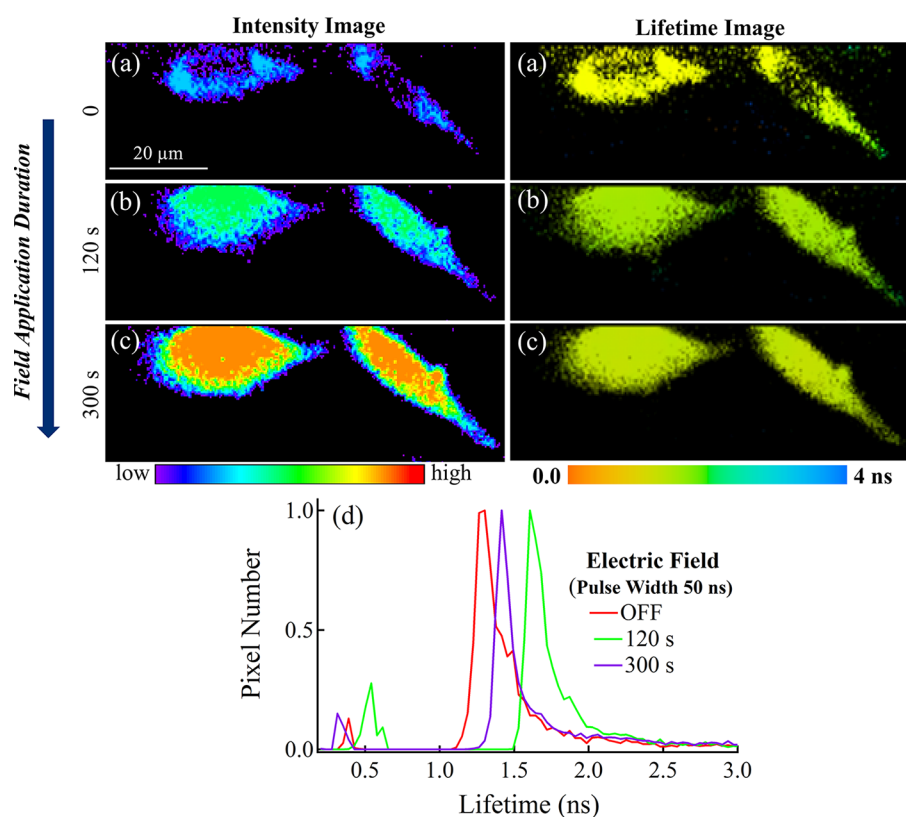
Figure 1. Autofluorescence intensity images (left) and the corresponding lifetime images (right) of NADH in HeLa cells, observed before and after the application of an electric field having a strength of 45 kV cm^{-1} and a repetition rate of 1 kHz, with application durations of 120 and 300 s, respectively (from top to bottom). The pulse width of the electric field was 50 ns. The histograms of the autofluorescence lifetime of the images of (a–c) are shown in (d). Electric field was not applied during the image measurements.

processes.[17−20] Several approaches regarding electric fields have been demonstrated to manipulate the cell interior, but the effects of PEFs on intracellular processes are not fully understood. The responses of individual cells undergoing physiological and biochemical activation and/or changing processes are quite heterogeneous in time and space. Moreover, measurements of these physical parameters under bulk conditions with conventional physiological and biochemical methods often fail to reveal the intracellular kinetics and subcellular dynamics that are involved. However, it is important to understand how cells actually work under these specific conditions. Autofluorescence microscopy (i.e., autofluorescence intensity and lifetime imaging) is one of the most useful and robust noninvasive techniques for evaluating the subcellular activity of individual cells undergoing different physiological and biochemical changes.[21−24]

In our previous study,[25] fluorescence lifetime and intensity images of enhanced green fluorescent protein (EGFP) demonstrated the effects of PEFs on HeLa cells expressing EGFP. After the application of PEFs with a 50 ns pulse width and a 40 kV cm^{-1} strength, we measured the cell morphological changes and the EGFP fluorescence lifetime reduction. Furthermore, we detected the loss of plasma membrane asymmetry by assessing the redistribution of phosphatidylserine (PS) to the outer layer of the plasma membrane. We concluded that apoptosis is induced by the application of nanosecond PEFs (nsPEFs). However, we did not completely understand the mechanism of the observed field-induced apoptosis in these cells. In addition, these experiments were performed only with applied electric fields having a pulse width of 50 ns.

The electrical model of biological cells predicts that electric fields will interact with intracellular structural proteins without affecting the outer cellular membrane, as long as electric fields with a pulse width (t) that is shorter than the charging time of the outer membrane (τ_c) are applied. In the cases where $t \gg \tau_c$, for example, no field effect would be expected in intracellular organelles, although some changes or heating effects in the outer plasma membrane may be expected.[26] In contrast, the effects of electric fields on intracellular organelles and proteins are expected when t is much smaller than τ_c of the outer membrane. If electric pulses whose width is shorter than τ_c of the outer membrane are applied with an amplitude larger than that of the voltage across the subcellular membrane, it is expected that the PEF will cause significant effects on the intracellular function and dynamics. This selective nature of electric fields with respect to the charging time of the membrane will hold true for both the extracellular membrane and the subcellular organelle membranes, which may induce selective and controlled effects from PEFs on subcellular organelles and signaling.

In this study, we used a homemade bioelectric chip fabricated on a culture glass slide prepared by the UV photolithographic method.[25] The chip is available for the application of PEFs in any kind of living cells/tissues (size ≤100 μm) and for the real-time monitoring of the effects of PEFs on living cells/tissues. The aim of this study was to activate the physiological and biochemical intracellular mechanisms that take part in the process of programmed cell death to better understand the biological effects of PEFs through the noninvasive detection of intracellular coenzymes in the form of autofluorescence

measurements of NADH. The visualization of intracellular NADH by fluorescence intensity and lifetime microscopy makes it possible to distinguish intracellular organelles such as mitochondria and cytosol, which take part in glucose metabolism for ATP production, from other nonfluorescent organelles without inducing exogenous chromophores. To examine the pulse-width dependence of the applied electric-field effect, electric fields with square pulse widths of 10, 20, 30, and 50 ns were applied to living HeLa cells; responses were monitored using NADH autofluorescence intensity and lifetime microscopy.

■ RESULTS

Autofluorescence intensity and lifetime images of endogenous NADH in HeLa cells were observed before and after the application of PEFs with a pulse width of 50 ns, strength of 45 kV cm^{-1}, and a repetition rate of 1 kHz. The results are shown in Figure 1. The intensity image shows the natural distribution of NADH within the cells. Because of the very weak fluorescence signal, the nucleus can be differentiated from other NADH-fluorescent organelles when the electric field is not applied, and the intensity of mitochondria-associated NADH appears dominant. As shown in Supporting Information (Figure S1), the fluorescence decay profiles of NADH were fitted by assuming a biexponential decay, that is, $\sum_i A_i \exp(-t/\tau_i)$, where A_i and τ_i are the pre-exponential factor and the lifetime of the ith component, respectively, that is, $i = 1$ and 2. A third component whose lifetime is longer than 10 ns exists, but this component was neglected in the present analysis because the contribution of this weak emission was very small.[23] The histogram of the average fluorescence lifetime, that is, $\sum_i A_i \tau_i / A_i$ in each pixel, is also shown in Figure 1. This is the amplitude average lifetime that a fluorophore would have if it had the same steady-state fluorescence as the fluorophore with several lifetimes.[27] The decay profiles show both fast- and slowly decaying components whose lifetimes are ∼460 ps and ∼3.9 ns, respectively, before the application of the electric field (see Table 1 and Figure S1). Note that the analysis whose results are shown in Table 1 was carried out by assuming a biexponential decay for the summation of the decay profiles of

all of the pixels. These quickly and slowly decaying components were assigned to two different protein-bound species of NADH in HeLa cells, loosely protein-bound NADH and tightly protein-bound NADH, respectively, as opposed to free and protein-bound NADH. As shown in our previous paper,[23] the shift of the picosecond time-resolved fluorescence due to the existence of free NADH was not observed in HeLa cells, suggesting that the classification between loosely and tightly protein-bound proteins may be appropriate in the present case.

Control experiments were done with a biochip to confirm that the observed changes in intensity and lifetime of NADH autofluorescence in HeLa cells, as well as structural changes, resulted from the application of the PEF and not from any external factors such as laser light irradiation or measurement conditions. Thus, time-lapse measurements of autofluorescence images of NADH in HeLa were performed under the same experimental conditions but without the application of the electric field. Changes in cell morphology and autofluorescence lifetime were not observed without the application of the electric field, even after 1 h photoirradiation under a similar irradiation light intensity, as shown in Figure S2. These results indicate that the observed changes in the fluorescence properties of NADH and in cellular morphology were induced by the application of the nsPEFs.

The application of a 50 ns PEF enhanced the intensity of NADH fluorescence and also changed the intracellular intensity distribution in each cell; the increased intensity extended over the entire region of the cell, and the nucleus could not be distinguished from other organelles after the application (see Figure 1). The intensity was estimated by integrating the decay profile at each pixel, and these intensities were summed for all of the cells observed in the images to estimate the total intensity before and after the application of electric fields. Along with the change in intensity, the average lifetime of NADH also changed, that is, from ∼1.3 ns (before application) to ∼1.6 ns (after the 120 s application) (see Table 1 and the histogram in Figure 1). However, further application of 180 s, that is, a total field application duration of 300 s, induced a decrease in the lifetime to ∼1.4 ns, although the intensity became stronger. We also noticed that the longer application of the 50 ns PEF induced swelling in the cellular structure, as shown in Figure S3.

Similar experiments with different pulse widths of 30, 20, and 10 ns were carried out with the same repetition rate, field strength, and application duration. These results are shown in Figures 2−4. It was then found that the effect of nsPEFs on the NADH fluorescence intensity depended on the pulse width of the applied electric field. As mentioned, the NADH fluorescence intensity increases after the application of the electric field of 50 ns pulse width. Application of electric fields with a much shorter pulse width of 10 ns, however, led to a slight decrease in NADH fluorescence intensity both after the 120 s application and after the 300 s application. Plots of fluorescence intensity obtained after the application of nsPEFs relative to the intensity obtained before the application of the electric field are shown in Figure 5a for different pulse widths, as a function of the field application duration. The intensity observed with a 30 ns pulse width shows the application duration dependence similar to that with a 50 ns pulse width; the intensity monotonically increased with increasing application duration, although the magnitude of the increase is smaller than that with the 50 ns pulse width (see Figure 5a). With a 20 ns pulse width, the fluorescence intensity slightly increased after

Table 1. Results of the Analysis of the NADH Fluorescence Decay Profiles Observed before and after the Application of PEF^a

pulse width (ns)	field application duration (s)	τ_{av} (ns)	τ_I (ns)	τ_{II} (ns)
50	0	1.29	0.46 (0.76)	3.90 (0.24)
	120	1.58	0.63 (0.70)	3.81 (0.30)
	300	1.37	0.38 (0.59)	2.80 (0.41)
	0	1.32	0.40 (0.73)	3.80 (0.27)
30	120	1.90	0.83 (0.65)	3.90 (0.35)
	300	1.58	0.48 (0.57)	3.04 (0.43)
	0	1.31	0.35 (0.67)	3.25 (0.33)
20	120	1.99	0.70 (0.68)	4.72 (0.32)
	300	1.72	0.61 (0.64)	3.68 (0.36)
	0	1.26	0.35 (0.72)	3.60 (0.28)
10	120	1.99	0.79 (0.68)	4.53 (0.32)
	300	1.71	0.65 (0.65)	3.68 (0.35)

^{a}Lifetimes of the fast- and slowly decaying components, that is, τ_I and τ_{II}, are shown, together with the pre-exponential factor in parentheses and the average lifetime, τ_{av}. The uncertainty is estimated to be 10%.
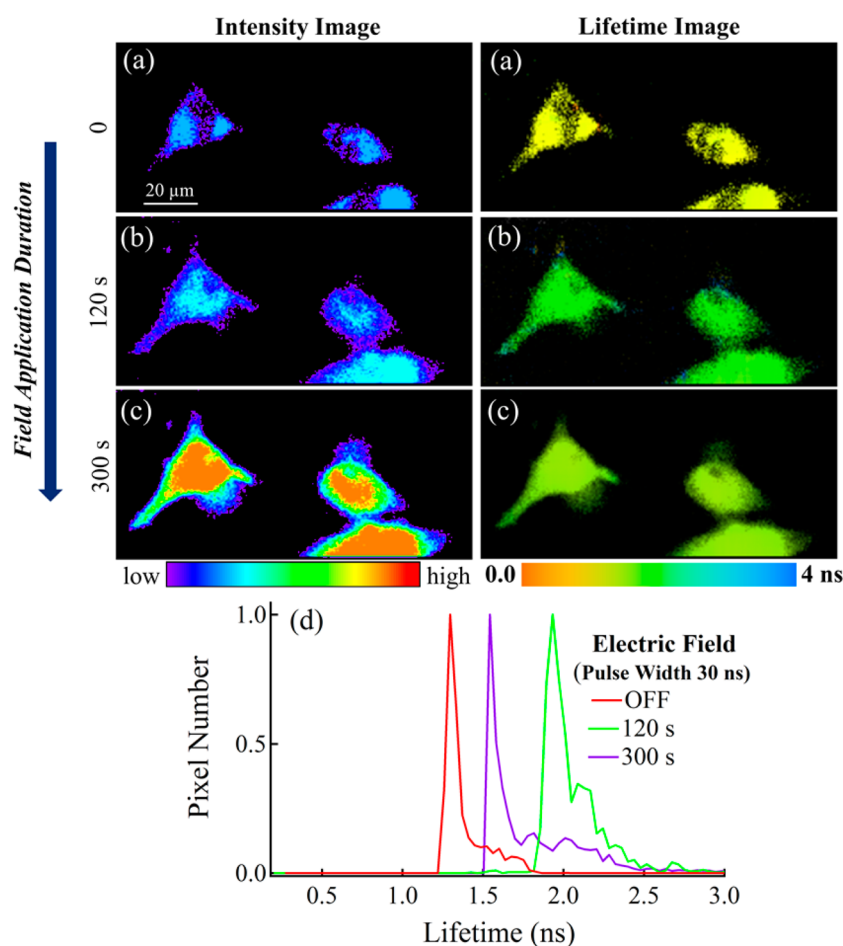
Figure 2. Autofluorescence intensity images (left) and the corresponding lifetime images (right) of NADH in HeLa cells, observed before and after the application of an electric field having a strength of 45 kV cm^{-1} and a repetition rate of 1 kHz with the application duration of 120 and 300 s, respectively (from top to bottom). The pulse width of the electric field was 30 ns. The histograms of the autofluorescence lifetime of the images of (a−c) are shown in (d). Electric field was not applied during the image measurements.

the 120 s application, but the intensity is nearly the same after the 300 s application. Thus, the magnitude of the field-induced increase in NADH fluorescence intensity appears to decrease with smaller pulse widths of the applied electric field, and the field effect on intensity changes from enhancement to quenching as the pulse width becomes smaller from 50 to 10 ns.

When the same field strength and the same repetition rate are used, the electrical energy produced by the applied electric field is proportional to the pulse width, and the total energy produced by a 50 ns pulse width is fivefold higher than that produced by a 10 ns pulse width. As shown in Figure 5, however, it is clear that the difference among the various pulse widths, with regard to the duration dependence of field-induced intensity changes, does not come from the difference in the total electric power of the applied electric field. There is a clear gap between 30 and 20 ns regarding the pulse-width dependence of the field effect on the fluorescence intensity, which may be related to the nature of the effects of nsPEFs on the intracellular function.

Regarding the field-induced changes in fluorescence lifetime, a similar trend was observed with any pulse width in the range of 10−50 ns, in contrast to the field effect on intensity. As shown in Figures 1d−4d, the average lifetime became longer in the first step, that is, after the first application of the PEF for 120 s. After the next 180 s application, the lifetime became

shorter, but it was still longer than that observed before the application of the electric field. The lifetime and pre-exponential factor of each of the fast- and slowly decaying components observed before and after the application of electric fields with pulse widths of 10, 20, and 30 ns are also shown in Table 1, together with the results for 50 ns. This analysis was carried out by assuming a biexponential decay for the summation of all of the decay profiles collected from different pixels in the image, which is the same as the one used for the evaluation of the lifetime before and after the application of the electric field having a 50 ns pulse width. In every case, the average lifetime is very similar to the peak lifetime of the histogram shown in Figures 1d−4d. As shown in Table 1, the magnitude of the change in lifetime after the application of 120 s has a tendency to decrease with increasing pulse width of the applied field. This behavior is clearly seen in Figure 5b. The magnitude of the reduction in lifetime after the 300 s application was rather small when the shorter pulse widths were used; the difference in the lifetime between the 120 and 300 s applications relative to the difference between the 0 and 120 s applications was smaller with a pulse width of 10 or 20 ns than that with a pulse width of 30 or 50 ns. For example, this ratio was 0.38 and 0.72, respectively, for pulse widths of 10 and 50 ns.

The lengthening of the average fluorescence lifetime after the application of the electric field of 120 s mainly resulted from
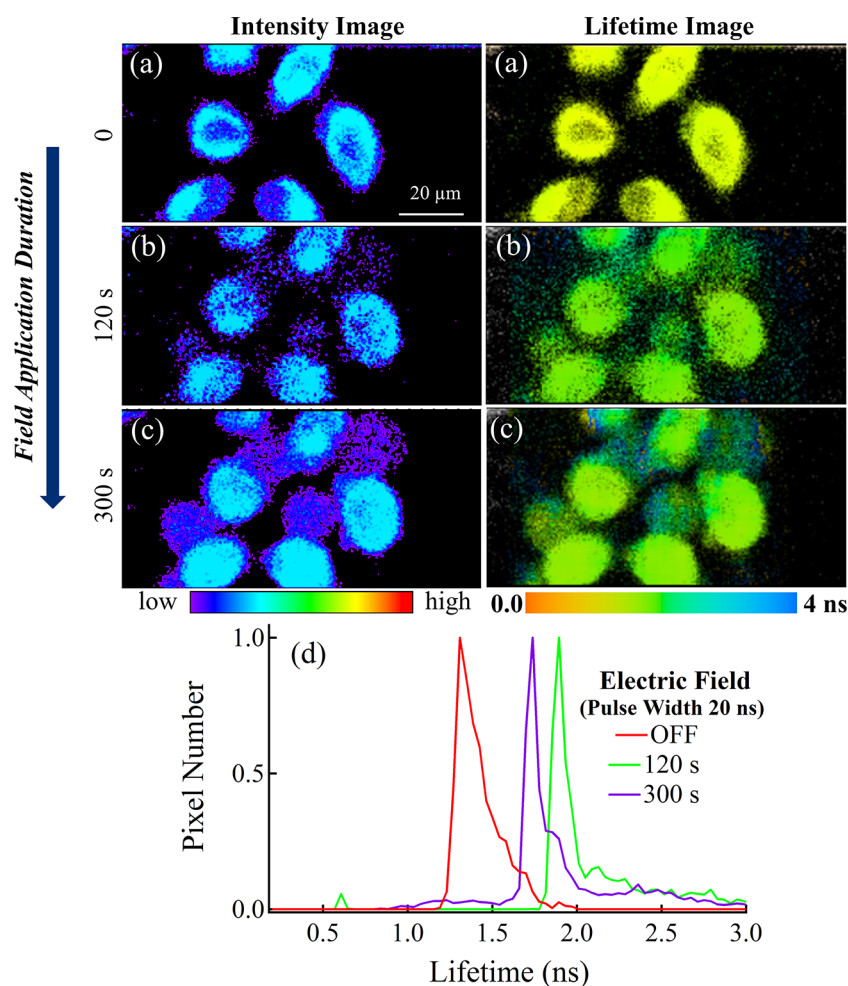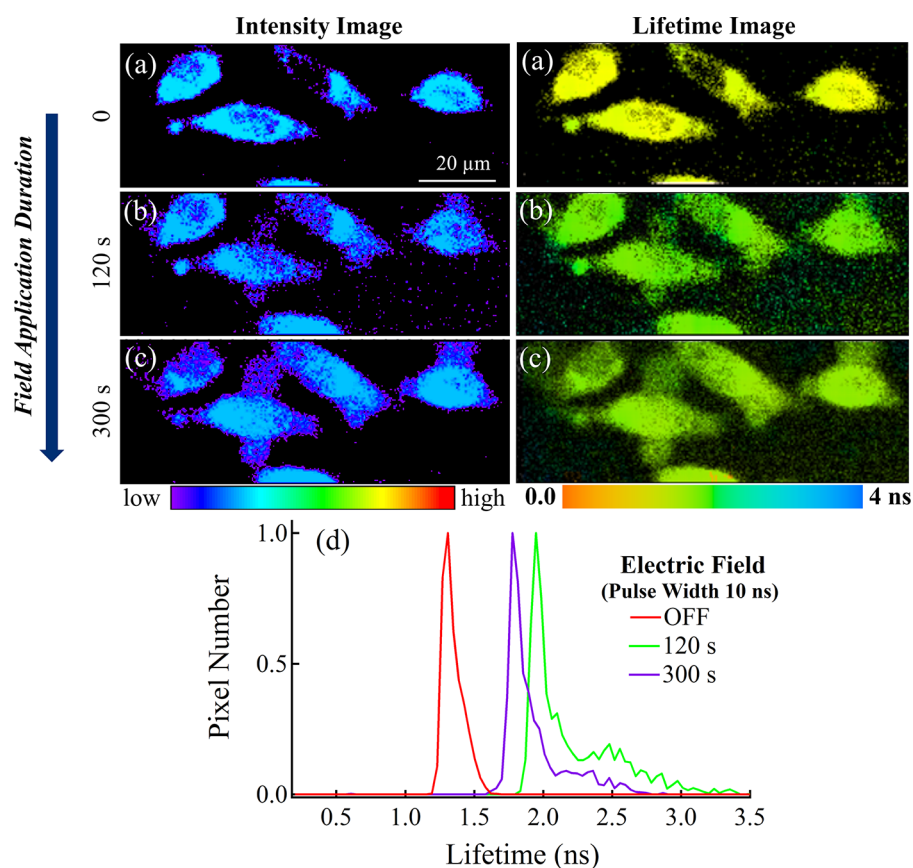
Figure 3. Autofluorescence intensity images (left) and the corresponding lifetime images (right) of NADH in HeLa cells, observed before and after the application of an electric field having a strength of 45 kV cm^{-1} and a repetition rate of 1 kHz with the application duration of 120 and 300 s, respectively (from top to bottom). The pulse width of the electric field was 20 ns. The histograms of the autofluorescence lifetime of the images of (a−c) are shown in (d). Electric field was not applied during the image measurements.

the lengthening of the lifetime of the fast-decaying component in every pulse width, as shown in Table 1. Moreover, the difference in the average lifetime after the 120 s application between the short pulse width (10 or 20 ns) and the large pulse width (30 or 50 ns) came from the difference in the lifetime of the slow component; the lifetime of the slow component became larger with the application of electric fields of a 10 or 20 ns pulse width compared to that of electric fields of a 30 or 50 ns pulse width. After the 300 s application, the lifetime of the fast component became shorter, resulting in a shorter average lifetime for the 300 s application than for the 120 s application. With 10 or 20 ns pulse width, the pre-exponential factor of the slow component increased after the 300 s application, and the lifetime of the fast component was still longer than that before the application of the electric field. In the case of 50 or 30 ns pulse width, the lifetime of the fast-decaying component after the 300 s application was similar to the one observed before the application of the electric field, and the difference in the average lifetime after the 300 s application and before the application came from the difference in the pre-exponential factor of the slowly decaying component.

The experimental results of the effects of nsPEFs on the NADH fluorescence intensity and lifetime in HeLa cells are summarized as follows: (1) when the pulse width is as large as 50 or 30 ns, the fluorescence intensity increases and distributes over the entire cell with application of the electric field; (2) when the pulse width is smaller than some threshold, the fluorescence intensity is nearly constant or slightly de-enhanced by nsPEF application; (3) the fluorescence lifetime becomes longer by applying nsPEF of any pulse width in the range of 10 − 50 ns; (4) after the 300 s application, the fluorescence lifetime is shorter than that observed after the 120 s application but still longer than that before the field application; (5) the field-induced lengthening of the fluorescence lifetime after the 120 s application mainly results from the lengthening of the lifetime of the fast-decaying component in the case of 30 or 50 ns pulse width, whereas the lengthening of both the fast- and slowly decaying components leads to the lengthening of the average lifetime for 10 or 20 ns pulse width; (6) the field-induced increase in the pre-exponential factor of the slow component plays an important role in showing the difference with a 30 or 50 ns pulse width between the lifetimes before the application and after the 300 s application, whereas both the lifetime of the fast component and the pre-exponential factor of the slow component change after the 300 s application for 10 or 20 ns pulse width.

Figure 4. Autofluorescence intensity images (left) and the corresponding lifetime images (right) of NADH in HeLa cells, observed before and after the application of an electric field having a strength of 45 kV cm^{-1} and a repetition rate of 1 kHz with the application duration of 120 and 300 s, respectively (from top to bottom). The pulse width of the electric field was 10 ns. The histograms of the autofluorescence lifetime of the images of (a−c) are shown in (d). Electric field was not applied during the image measurements.

■ DISCUSSION

When the pulse width of the applied electric field is sufficiently small, the voltage across the membrane is negligible, resulting in the deep penetration of the applied electric field into intracellular organelles. In contrast, when the pulse width of the applied electric field is large enough in comparison to the charging time τ_c, the voltage across the membrane becomes very large, resulting in the breakdown of the cell membrane and production of holes on the cell surface. In a single-shell model,[28] τ_c is given as follows

$$\tau_c = \left[\left(\frac{1 + 2V}{1 - V}\right)\frac{\rho_1}{2} + \rho_2\right]C_m r \tag{1}$$

where V is the volume fraction of cells in the suspension, ρ_1 and ρ_2 are external and internal resistivity, respectively, C_m is the capacitance of the membrane per unit area, and r is the radius of the spherical cell.

By assuming that a spherical cell has a radius of 10 μm, ρ_1 and ρ_2 of 100 Ω cm, membrane capacitance of 1 μF cm^{-2}, and a volume fraction much smaller than one, the charging time is estimated to be 150 ns, which is much larger than the pulse width of the applied electric field used in this study. In this case, the electric-field effect observed in this study is considered to result mainly from the field effect on the intracellular function.

In addition to the change in intensity and lifetime of NADH autofluorescence, structural changes of HeLa cells are induced by the application of the electric field. The cellular blebbing

induced by the applied electric field was more dominant with a short pulse width of 10 or 20 ns than with 50 or 30 ns pulse width (see Figures S3 and S4). It is conceivable from the discussion using the above eq 1 that electric fields with shorter pulse widths penetrate more deeply into mitochondria through membranes and induce direct modifications of the DNA structure and biochemical processes, which may affect other signal proteins, subcellular organelles, and/or biochemical processes.

As mentioned previously, apoptosis was induced in HeLa cells expressing EGFP by applying nsPEF with a pulse width of 50 ns and a strength of 40 kV cm^{-1}.[25] Fluorescence of EGFP is much stronger than the autofluorescence of NADH, and so the field-induced change in the cellular structure can be clearly observed in EGFP-expressing HeLa cells. Such a structural change is also shown in Figure S5. nsPEF-induced apoptosis has also been reported in other cells, including Jurkat cells.[18,29,30] Our results show that the effects of nsPEF on the intensity and lifetime of NADH autofluorescence in HeLa cells are similarly ascribed to electric-field-induced apoptosis. In the present measurements of NADH autofluorescence, EGFP has not been expressed in HeLa cells, and the autofluorescence of NADH has been monitored. Irrespective of the presence of EGFP, we can conclude that apoptosis is induced by the application of nsPEF in HeLa cells. Apoptosis is traditionally defined by physiological changes, such as cell shrinkage, cell surface blebbing, and DNA fragmentation. Accordingly, some
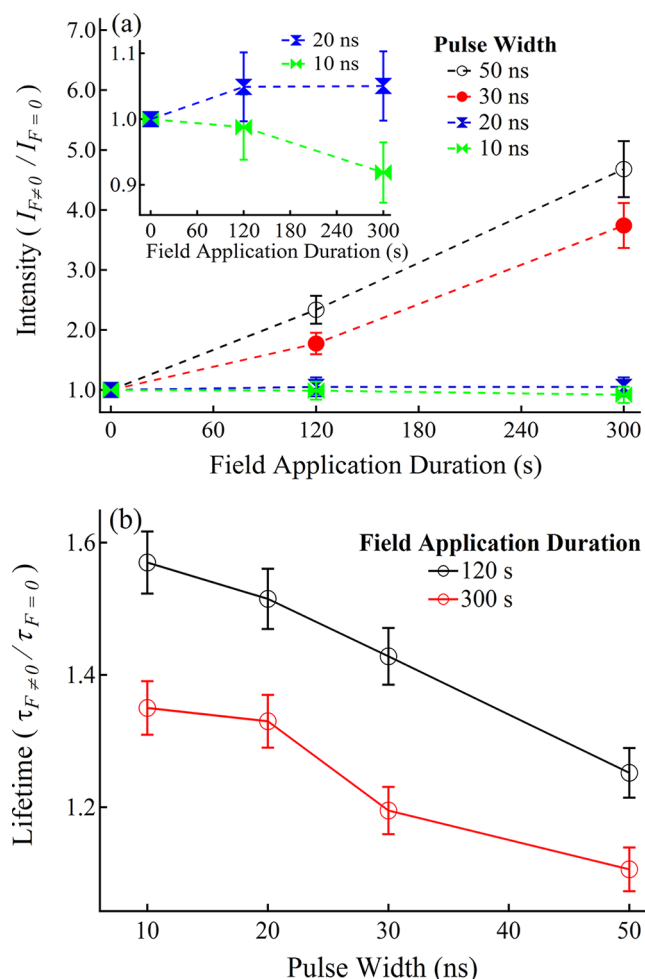
Figure 5. (a) Plots of the ratio of the autofluorescence intensity of NADH in HeLa cells after the application of an electric field ($I_{F\neq0}$) relative to the intensity before the application ($I_{F=0}$) as a function of field application duration, with different pulse widths of 10, 20, 30, and 50 ns, a field strength of 45 kV cm^{-1}, and a repetition rate of 1 kHz. (b) Plots of the ratio of the fluorescence lifetime of NADH after the application of an electric field ($\tau_{F\neq0}$) relative to the lifetime before the application ($\tau_{F=0}$), as a function of the pulse width of the applied electric field. An expanded view of the intensities for 10 and 20 ns pulse widths is also shown in the inset of (a). The intensity was estimated by integrating the intensities of all of the pixels, and the lifetime was obtained from the peak in the histogram.

of these physiological changes were observed in this study, as mentioned above.

Measurements of NADH autofluorescence lifetime in HeLa cells were performed with STS, a known inducer of apoptosis.[1−5,31] Time lapse of the NADH fluorescence lifetime following the addition of STS showed the same trends as those observed in the present results of the pulsed electric-field effect; after the addition of STS, the autofluorescence lifetime of NADH increases followed by decreases in a stepwise manner.[31] As shown in Figure S6, the results reported above have been reconfirmed in the present study. Thus, our findings, while showing that the lifetime of NADH fluorescence increases after the application of an electric field, also support that apoptosis is induced by the application of nsPEF in HeLa cells. Similarly to previous experiments with STS, the NADH fluorescence lifetime becomes shorter after the 300 s application in comparison with the 120 s application, as shown in Figures

1−4 and S6. The nonmonotonic time-lapse dependence of the field-induced increase in the fluorescence lifetime of NADH following the application of an electric field may indicate a multistep process of apoptosis under the application of PEFs. In the case of STS-induced apoptosis, the fluorescence intensity of NADH increased immediately just after the addition of 1 μM STS and continued to increase until a certain time (~70 min). After that, the intensity saturated, as shown in Figure S6, which is different from the field effect on the NADH fluorescence intensity given in Figure 5, particularly with the short pulse application.

In terms of the origin of the field-induced increase of fluorescence intensity, two possibilities can be considered. The first is a field-induced increase in fluorescent NADH concentration; the second is a field-induced increase in the fluorescence quantum yield of NADH. The fact that the average fluorescence lifetime becomes longer in the presence of the electric field indicates that the nonradiative decay at the emitting state becomes slower in the presence of the electric field, that is, the quantum yield of the NADH fluorescence increases after the application of the electric field. As shown in Figure 5, the fluorescence intensity becomes higher by a factor of more than 2 and 4 with a pulse width of 50 ns for the application duration of 120 and 300 s, respectively, whereas the increase in the lifetime is less than twice in both cases. These results show that the field-induced increase in intensity cannot be explained only by the increase in the fluorescence quantum yield. Therefore, there is no doubt that the field-induced increase in fluorescence intensity observed with a pulse width of 30 or 50 ns mainly results from the field-induced increase in the number of fluorophores, that is, the concentration of the emitting species of NADH is increased by the application of the PEFs. When the pulse width is as short as 10 or 20 ns, and the field-induced change in fluorescence intensity is very small, the concentration of the emitting species of NADH is not so sensitive to the applied electric field. In every pulse width, however, the fluorescence quantum yield is considered to increase in the presence of electric fields because the fluorescence lifetime becomes longer in their presence. As the pulse width becomes smaller, the ratio of the fluorescence lifetime after the application of nsPEF relative to the one before application becomes larger (see Figure 5b). These results suggest that the field-induced enhancement of the fluorescence quantum yield becomes larger with decreasing pulse width, that is, the nonradiative decay rate becomes slower with the application of nsPEF, and it is more prominent as the pulse width becomes smaller. The decrease in the nonradiative decay rate may indicate a shift in the population of proteins to which cellular NADH is strongly bound, consistent with a metabolism that is more efficient in ATP production. The field-induced change in the fluorescence lifetime of NADH is considered to arise from the physical effect: Intermolecular interactions of NADH with surrounding amino acids of protein may be changed by the application of electric fields, as an irreversible process. In fact, the change in protein structure was reported to be induced by nsPEF using ricin,[32] that is, the secondary structure of ricin was slightly changed by nsPEF, resulting in the reduction of the toxicity of ricin. We have previously shown that the fluorescence lifetime of NADH has a tendency to increase with decreasing polar environment around NADH, and the increase in the lifetime with binding to a protein can also be explained in terms of the decrease in the hydrophilicity of NADH.[33] The present results also reflect the change in the

polar environment around NADH, which can be considered to arise from the change in the interaction between NADH and a protein.

The fact that the NADH fluorescence spreads diffusely throughout the cell after the application of nsPEF indicates that pores are opened in the inner mitochondrial membranes, that is, the so-called mitochondrial permeability transition pore (MPTP) complex, which may induce apoptosis, is generated by the application of nsPEF,[34] particularly when the pulse width of the applied electric field is as large as 50 or 30 ns. Through the MPTPs produced in the inner and outer mitochondrial membranes, NADH probably spreads into the protoplasm from mitochondria. Membrane damage causes the leakage of coenzymes such as NADH from mitochondria and their diffusion into all parts of the cell, including the nucleus.[35] With a large pulse width, both apoptosis and necrosis may be initiated.[36] If only necrosis occurs, however, the fluorescence lifetime of NADH is considered to be unaffected by the applied electric field, as demonstrated by H_2O_2-induced necrosis.[31] Therefore, it is likely that apoptosis is surely induced by the applied electric fields with pulse widths of 50 and 30 ns, although the primary process of necrosis cannot be excluded completely. In fact, a similar spread of NADH fluorescence throughout the cell during early apoptotic stages has been reported in high-NaCl-induced apoptosis of mIMCD3 cells.[37] As the pulse width of the applied electric field becomes smaller, the redistribution of the NADH fluorescence intensity is inconspicuous, suggesting that the MPTP is induced by the electric field whose pulse width is larger than some threshold. Even with the short pulse width of 10 or 20 ns, the field-induced lengthening of the lifetime of NADH fluorescence was observed, indicating field-induced apoptosis in HeLa cells with short pulse widths of 10 and 20 ns.

As mentioned, the fluorescence lifetime shows a similar field effect in every pulse width in the range of 10−50 ns, but the fluorescence intensity shows different field dependence, that is, the field effect on the fluorescence intensity remarkably depends on the pulse width of the applied nsPEF. The intensity is largely enhanced by electric fields with a pulse width of 50 or 30 ns, whereas the field effect on the intensity is very small with a pulse width of 10 or 20 ns. Furthermore, with 10 ns, the intensity decreases after the application of electric fields. The energy saved in mitochondrial NADH is transferred to an electrochemical proton gradient that is necessary to drive the phosphorylation of ADP to ATP. The electron transport process starts with the oxidation of mitochondrial NADH to NAD^+, and so the redox ratio of NADH/NAD^+ can be regarded as an indicator of cellular metabolism.[38] The autofluorescence of NADH directly reflects the cellular metabolic state because the oxidation of NADH to NAD^+ via the electron transport chain results in a characteristic loss of the NADH fluorescence signal. As a potential origin of the field effect on fluorescence intensity with 50 or 30 ns pulse width (i.e., the field-induced increase in the concentration of fluorescent NADH), the depletion of energy metabolism in mitochondria from the disruption of electron transport should be considered.[1] On the basis of the measurements of the cytosolic ATP level in intact cells throughout the apoptotic process, apoptotic stimuli such as STS and TNF-α were found to induce significant enhancement of ATP levels, and it was suggested that an elevation of cytosolic ATP level is a requisite to the apoptotic cell death process.[39] If so, the field-induced enhancement in NADH fluorescence intensity would not come

from the field-induced increase in the ratio of NADH/NAD^+ but, rather, from the number of NADH molecules probably generated in the tricarboxylic acid cycle, which may be significantly increased by the application of PEFs with 50 or 30 ns pulse width.

Short pulses (10 ns) were more effective in inducing membrane blebbing compared to long pulses (50 ns) (cf. Figures S3 and S4). As mentioned, the effect of the PEF on subcellular membranes depends on the charging time of the subcellular membranes. If the pulse width of the applied electric field is shorter than the charging time of the subcellular membrane, the electric field can pass through the subcellular organelle membrane. Even when the charging time of the mitochondrial inner membranes is longer than 20 ns, the short pulses of 10 and 20 ns may pass through the outer and inner membranes of mitochondria and activate or modify the proteins inside the mitochondria very efficiently. The activation or modification process may then lead to efficient apoptotic cell death. The present results suggest that the nature of the apoptosis induced by the short pulses of 10 and 20 ns is different from that induced by the long pulses of 30 and 50 ns.

If a change in mitochondrial membrane permeability is essential for apoptosis,[40] mitochondria outer-membrane permeabilization (MOMP) may be induced by the application of the PEF, and apoptotic factors such as cytochrome c and an apoptosis-inducing factor may be released into the cytosol.[41] This would be true in the cases of 10 or 20 ns pulse width, where it is unlikely that MPTP is important. It is well known that the release of cytochrome c from mitochondria plays an important role in apoptosis. This mechanism is mainly controlled by the Bcl-2 family of proteins, such as Bcl-2 (antiapoptotic) and Bak & Bax (proapoptotic), which are located between the inner and outer membranes of mitochondria.[42] It seems that nsPEFs either reduce the expression of Bcl-2 or increase the expression of Bak and Bax. The disruption of the mitochondrial membrane and the formation of pores by the PEF should release cytochrome c from mitochondria. Therefore, MOMP may play an important role in field-induced apoptosis by nsPEF whose width is as short as 10 or 20 ns, irrespective of the caspase-dependent and -independent mechanisms.[41,43] Unfortunately, in the present experiments it is not known whether the calcium ion is required for nsPEF-induced apoptosis.[18]

It is well recognized that mitochondria are a major source of reactive oxygen species (ROS), such as single oxygen ($^1O_2$) and anionic superoxide (O_2^-), and the production of $^1O_2$ and O_2^- increases during the apoptosis.[7−9,44] For example, it has been shown that STS-induced apoptosis in HeLa cells is mainly mediated by the anionic superoxide (O_2^-).[7] Thus, it is conceivable that ROS production due to electron leakage in the respiratory chain may induce the quenching of NADH autofluorescence.[45] The dynamic quenching of fluorescent NADH by ROS may be supported by the field-induced changes in NADH intensity and lifetime under the application of PEFs. The lifetimes of both fast and slow components observed after the 300 s application were shorter than the corresponding ones observed after the first 120 s application (see Table 1). However, the field-induced quenching of NADH fluorescence observed after the application of a 10 ns PEF may be interpreted in terms of static quenching of fluorescent NADH by ROS. At the moment, it is not certain whether the concentration of NADH is significantly enhanced by the

application of electric fields with pulse widths as short as 10 or 20 ns.

CONCLUSIONS

Autofluorescence lifetime images as well as intensity images of the endogenous fluorophore of NADH were recorded in HeLa cells, before and after the application of nsPEFs with a strength of 45 kV cm^{-1}, a repetition rate of 1 kHz, and a pulse width of 10, 20, 30, or 50 ns. In every case, the fluorescence lifetime of NADH became longer by applying nsPEFs, and further application induced a decrease in the lifetime. This behavior was very similar to the time-lapse dependence of the fluorescence lifetime of NADH in HeLa cells observed after the addition of STS, a well-known apoptosis inducer. Morphological changes in the cell structure were also induced by the application of PEFs. These results show that apoptosis is induced in HeLa cells by the application of nsPEFs having a pulse width in the range of 10−50 ns. The magnitude of the field-induced change in lifetime, as well as the field-induced change in morphology, became larger when the pulse width of the applied electric field was reduced. These findings indicate that field-induced apoptosis becomes more efficient with decreased pulse widths of the applied electric fields, with the field strength remaining the same, likely because electric fields with a short pulse width can penetrate deeply into the mitochondria and initiate apoptosis more efficiently. When the pulse width of the applied electric field is as large as 30 or 50 ns, the fluorescence intensity increases with the applied electric field and its magnitude monotonically increases with increasing application duration. Furthermore, the intensity distribution spreads over the entire region of each cell. MPTP induced by the applied electric field probably plays a significant role in the initiation of apoptosis with a pulse width as large as 50 or 30 ns. As the pulse width becomes smaller, the magnitude of the field-induced change in intensity becomes smaller, and the intensity decreases when the pulse width is as small as 10 ns. With such a short pulse width, MOMP, which induces a release of apoptotic factors and activates the apoptotic process, may occur. At the same time, ROS may be produced by the field-induced leakage of electrons from the respiratory chain during electron transfer to molecular oxygen, and the produced ROS may induce the quenching of NADH fluorescence. Fluorescence lifetime and intensity images observed before and after the application of PEFs suggest that nsPEF-induced apoptosis could be caused by two mechanisms depending on the applied nsPEF pulse width.

METHODS

Biochip Fabrication. Microchannel bioelectric chips were fabricated on microscopic cover glasses using the UV photolithographic method. Microwall arrays of microchannels were produced by SU-8, 2015 negative photoresist (Micro Chem) by the exposure of UV light.[25] After the chemical treatments, the array of photoresist microchannels could be produced. The Au layer was then deposited twice (35 nm each) at +30° and −30°, respectively, with respect to the substrate, to cover the sidewalls of the photoresist microchannels by helicon sputtering (MPS-4000c1/HC1; ULVAC, Japan). Finally, the resultant electrode microchannels were immersed in acetone for 10−15 min. The ultrasonic treatment was used to take out the gold film from the undesired area of the substrate. The width and depth of the microchannels were about 100 ± 1 and 20 ± 1 μm, respectively, as shown in Figure S7. The living cells

were cultured between the microchannels. In this study, nsPEFs having durations of 10, 20, 30, and 50 ns were applied with a voltage of 450 V and a load resistance of 50 Ω, which correspond to a field strength of 45 kV cm^{-1} for an interelectrode distance of 100 μm using a pulse generator (Avtech Electrosystems Ltd.). The internal field factor was taken as unity.

Cell Culture. HeLa cells were cultured in the fabricated biochips at 37 °C in Dulbecco's modified Eagle's medium (DMEM, D5796; Sigma) supplemented with 2×10^5 U dm^{-3} penicillin G, 200 mg of streptomycin sulfate, and 10% fetal bovine serum in a 5% CO_2 humidified atmosphere. The cell culture medium was replaced with calcium- and magnesium-free phosphate buffered saline medium just before the measurements.

Autofluorescence Intensity and Lifetime Imaging. Measurements of endogenous NADH intensity and lifetime images of cultured cells before and after the application of the PEFs were carried out by an inverted microscope (TE2000E; Nikon, Japan) through the objective lens (40×) using a time-correlated single photon counting system (SPC-830; Becker & Hickl GmbH).[25] The second harmonic output at 380 nm from a mode-locked Ti:sapphire laser (Tsunami, Spectra Physics, pulse duration of about 80 fs, repetition rate of 81 MHz) was used as the excitation light for NADH. The autofluorescence signal of NADH was detected using a microchannel-plate photomultiplier tube in the region of 447−460 nm. The analysis of the collected data was done with SPC image software (Becker & Hickl GmbH). The observed fluorescence decays were fitted by a convolution of the instrumental response function with a multiexponential decay.

Fluorescence images were initially observed before the application of the electric field, with two other image measurements taken to examine the electric-field effect. The PEFs with four different pulse widths of 10, 20, 30, and 50 ns with the same strength (45 kV cm^{-1}) and repetition rate of 1 kHz were used. The first image measurement was taken following the application of the above-mentioned electric field for 120 s. After that, the same PEF was further applied for 180 s and the second image measurement was taken, that is, the image measurements were done after field application duration of 120 and 300 s, respectively. The acquisition time of the images was fixed at 20 min in every case.

ASSOCIATED CONTENT

ⓢ Supporting Information

The Supporting Information is available free of charge on the ACS Publications website at DOI: 10.1021/acsomega.6b00090.

> Fluorescence decay profiles, fluorescence intensity and lifetime images for control experiments, fluorescence intensity images before and after the application of electric field, fluorescence intensity and lifetime images before and after the treatment by an apoptosis inducer, and illustration of fabrication of microelectrodes (PDF)

AUTHOR INFORMATION

Corresponding Author

*E-mail: nohta@nctu.edu.tw.

Notes

The authors declare no competing financial interest.

ACKNOWLEDGMENTS

REFERENCES

(1) Green, D. R.; Reed, J. C. Mitochondria and Apoptosis. *Science* **1998**, *281*, 1309−1312.

(2) Thornberry, N. A.; Lazebnik, Y. Caspases: Enemies Within. *Science* **1998**, *281*, 1312−1316.

(3) Hoppins, S.; Nunnari, J. Mitochondrial Dynamics and Apoptosis-the ER Connection. *Science* **2012**, *337*, 1052−1054.

(4) Friedman, J. R.; Nunnari, J. Mitochondrial Form and Function. *Nature* **2014**, *505*, 335−343.

(5) Susin, S. A.; Lorenzo, H. K.; Zamzami, N.; Marzo, I.; Snow, B. E.; Brothers, G. M.; Mangion, J.; Jacotot, E.; Costantini, P.; Loeffler, M.; Larochette, N.; Goodlett, D. R.; Aebersold, R.; Siderovski, D. P.; Penninger, J. M.; Kroemer, G. Molecular Characterization of Mitochondrial Apoptosis-Inducing Factor. *Nature* **1999**, *397*, 441−446.

(6) Kroemer, G.; Dallaporta, B.; Resche-Rigon, M. The Mitochondrial Death/Life Regulator in Apoptosis and Necrosis. *Annu. Rev. Physiol.* **1998**, *60*, 619−642.

(7) Shimizu, T.; Numata, T.; Okada, Y. A Role of Reactive Oxygen Species in Apoptotic Activation of Volume-Sensitive Cl⁻ Channel. *Proc. Natl. Acad. Sci. U.S.A.* **2004**, *101*, 6770−6773.

(8) Maeno, E.; Ishizaki, Y.; Kanaseki, T.; Hazama, A.; Okada, Y. Normotonic Cell Shrinkage Because of Disordered Volume Regulation is an Early Prerequisite to Apoptosis. *Proc. Natl. Acad. Sci. U. S. A.* **2000**, *97*, 9487−9492.

(9) Garcia-Perez, C.; Roy, S. S.; Naghdi, S.; Lin, X.; Davies, E.; Hajnoczky, G. Bid-induced Mitochondrial Membrane Permeabilization Waves Propagated by Local Reactive Oxygen Species (ROS) Signaling. *Proc. Natl. Acad. Sci. U.S.A.* **2012**, *109*, 4497−4502.

(10) Ito, T.; Oshita, S.; Nakabayashi, T.; Sun, F.; Kinjo, M.; Ohta, N. Fluorescence Lifetime Images of Green Fluorescent Protein in HeLa Cells During TNF-α Induced Apoptosis. *Photochem. Photobiol. Sci.* **2009**, *8*, 763−767.

(11) Kroemer, G.; Dallaporta, B.; Resche-Rigon, M. The Mitochondrial Death/Life Regulator in Apoptosis and Necrosis. *Annu. Rev. Physiol.* **1998**, *60*, 619−642.

(12) Baker, M. Nanoelectroporation. *Nat. Methods* **2011**, *8*, 996−997.

(13) Boukany, P. E.; Morss, A.; Liao, W.-C.; Henslee, B.; Jung, H. C.; Zhang, X.; Yu, B.; Wang, X.; Wu, Y.; Li, L.; Gao, K.; Hu, X.; Zhao, X.; Hemminger, O.; Lu, W.; Lafyatis, G. P.; Lee, L. J. Nanochannel Electroporation Delivers Precise Amount of Biomolecules into Living Cells. *Nat. Nanotechnol.* **2011**, *6*, 747−754.

(14) Xie, C.; Lin, Z.; Hanson, L.; Cui, Y.; Cui, B. Intracellular Recording of Action Potentials by Nanopillar Electroporation. *Nat. Nanotechnol.* **2012**, *7*, 185−190.

(15) Duan, X.; Gao, R.; Xie, P.; Cohen-Karni, T.; Qing, Q.; Choe, H. S.; Tian, B.; Jiang, X.; Lieber, C. M. Intracellular Recordings of Action Potentials by an Extracellular Nanoscale Field-Effect Transistor. *Nat. Nanotechnol.* **2011**, *7*, 174−179.

(16) Liu, D. S.; Astumian, R. D.; Tsong, T. Y. Activation of Na⁺ and K⁺ Pumping Modes of (Na, K)-ATPase by an Oscillating Electric Field. *J. Biol. Chem.* **1990**, *265*, 7260−7267.

(17) Song, B.; Gu, Y.; Pu, J.; Reid, B.; Zhao, Z.; Zhao, M. Application of Direct Current Electric Fields to Cells and Tissues in Vitro and Modulation of Wound Electric Field in Vivo. *Nat. Protoc.* **2007**, *2*, 1479−1489.

(18) Beebe, S. J.; Sain, N. M.; Ren, W. Induction of Cell Death Mechanisms and Apoptosis by Nanosecond Pulsed Electric Fields (nsPEFs). *Cells* **2013**, *2*, 136−162.

(19) Semenov, I.; Xiao, S.; Pakhomov, A. G. Primary Pathways of Intracellular Ca²⁺ Mobilization by Nanosecond Pulsed Electric Field. *Biochim. Biophys. Acta* **2013**, *1828*, 981−989.

(20) Nuccitelli, R.; Lui, K.; Kreis, M.; Athos, B.; Nuccitelli, P. Nanosecond Pulsed Electric Field Stimulation of Reactive Oxygen Species in Human Pancreatic Cancer Cells is Ca²⁺ -dependent. *Biochem. Biophys. Res. Commun.* **2013**, *435*, 580−585.

(21) Skala, M. C.; Riching, K. M.; Gendron-Fitzpatrick, A.; Eickhoff, J.; Eliceiri, K. W.; White, J. G.; Ramanujam, N. In Vivo Multiphoton Microscopy of NADH and FAD Redox States, Fluorescence Lifetimes, and Cellular Morphology in Precancerous Epithelia. *Proc. Natl. Acad. Sci. U.S.A.* **2007**, *104*, 19494−19499.

(22) Heikal, A. A. Intracellular Coenzymes as Natural Biomarkers for Metabolic Activities and Mitochondrial Anomalies. *Biomarkers Med.* **2010**, *4*, 241−263.

(23) Ogikubo, S.; Nakabayashi, T.; Adachi, T.; Islam, Md. S.; Yoshizawa, T.; Kinjo, M.; Ohta, N. Intracellular pH Sensing Using Autofluorescence Lifetime Microscopy. *J. Phys. Chem. B* **2011**, *115*, 10385−10390.

(24) Ohta, N.; Nakabayashi, T. Intracellular Autofluorescence Species: Structure, Spectroscopy, and Photophysics. In *Natural Biomarkers for Cellular Metabolism, Biology, Techniques, and Applications*; Ghukasyan, V. V., Heikal, A. A., Eds.; CRC Press: Boca Raton, 2014; Chap. 2, pp 41−64.

(25) Awasthi, K.; Nakabayashi, T.; Ohta, N. Application of Nanosecond Pulsed Electric Fields into HeLa Cells Expressing Enhanced Green Fluorescence Protein and Fluorescence Lifetime Microscopy. *J. Phys. Chem. B* **2012**, *116*, 11159−11165.

(26) Gowrishankar, T. R.; Weaver, J. C. An Approach to Electrical Modeling of Single and Multiple Cells. *Proc. Natl. Acad. Sci. U.S.A.* **2003**, *100*, 3203−3208.

(27) Sillen, A.; Engelborghs, Y. The correct use of "average" fluorescence parameters. *Photochem. Photobiol.* **1998**, *67*, 475−486.

(28) Schoenbach, K. H.; Joshi, R. P.; Kolb, J. F.; Chen, N.; Stacey, M.; Blackmore, P. F.; Buescher, E. S.; Beebe, S. J. Ultrashort Electrical Pulses Open a New Gateway Into Biological Cells. *Proc. IEEE* **2004**, *92*, 1122−1137.

(29) Beebe, S. J.; Fox, P. M.; Rec, L. J.; Somers, K.; Stark, R. H.; Schoenbach, K. H. Nanosecond Pulsed Electric Field (nsPEF) Effects on Cells and Tissues: Apoptosis Induction and Tumor Growth Inhibition. *IEEE Trans. Plasma Sci.* **2002**, *30*, 286−292.

(30) Vernier, P. T.; Li, A.; Marcu, L.; Craft, C. M.; Gundersen, M. A. Ultrashort Pulsed Electric Fields Induce Membrane Phospholipid Translocation and Caspase Activation: Differential Sensitivities of Jurkat T Lymphoblasts and Rat Glioma C6 Cells. *IEEE Trans. Dielectr. Electr. Insul.* **2003**, *10*, 795−809.

(31) Wang, H.-W.; Gukassyan, V.; Chen, C.-T.; Wei, Y.-H.; Guo, H.-W.; Yu, J.-S.; Kao, F.-J. Differentiation of Apoptosis from Necrosis by Dynamic Changes of Reduced Nicotinamide Adenine Dinucleotide Fluorescence Lifetime in Live Cells. *J. Biomed. Opt.* **2008**, *13*, No. 054011.

(32) Wei, K.; Li, W.; Gao, S.; Ji, B.; Zang, Y.; Su, B.; Wang, K.; Yao, M.; Zhang, J.; Wang, J. Inactivation of Ricin Toxin by Nanosecond Pulsed Electric Fields Including Evidences from Cell and Animal Toxicity. *Sci. Rep.* **2016**, *6*, 18781.

(33) Nakabayashi, T.; Islam, Md. S.; Li, L.; Yasuda, M.; Ohta, N. Studies on external electric field effects on absorption and fluorescence spectra of NADH. *Chem. Phys. Lett.* **2014**, *595−596*, 25−30.

(34) Weaver, J. C. Electropoation of Biological Membranes from Multicellular To Nano Scales. *IEEE Trans. Dielectr. Electr. Insul.* **2003**, *10*, 754−768.

(35) Morbidelli, L.; Monici, M.; Marziliano, N.; Cogoli, A.; Fusi, F.; Waltenberger, J.; Ziche, M. Simulated Hypogravity Impairs the Angiogenic Response of Endothelium by Up-Regulating Apoptotic Signals. *Biochem. Biophys. Res. Commun.* **2005**, *334*, 491−499.

(36) Halestrap, A. A Pore Way to Die. *Nature* **2005**, *434*, 578−579.

(37) Michea, L.; Combs, C.; Andrews, P.; Dmitrieva, N.; Burg, M. B. Mitochondrial Dysfunction in an Early Event in High-NaCl-Induced Apoptosis of mIMCD3 Cells. *Am. J. Physiol. Renal Physiol.* **2002**, *282*, F981−F990.

(38) Chance, B.; Cohen, P.; Jobsis, F.; Schoener, B. Intracellular Oxidation-Reduction States in Vivo. *Science* **1962**, *137*, 499−508.

(39) Zamaraeva, M. V.; Sabirov, R. Z.; Maeno, E.; Ando-Akatsuka, Y.; Bessonova, S. V.; Okada, Y. Cells Die with Increased Cytosolic ATP during Apoptosis: A Bioluminescence Study with Intracellular Luciferase. *Cell Death Differ.* **2005**, *12*, 1390−1397.

(40) Shimizu, S.; Konishi, A.; Kodama, T.; Tsujimoto, Y. BH4 domain of antiapoptotic Bcl-2 family members closes voltage-dependent anion channel and inhibits apoptotic mitochondrial changes and cell death. *Proc. Natl. Acad. Sci. U.S.A.* **2000**, *97*, 3100−3105.

(41) Lakhani, S. A.; Masud, A.; Kuida, K.; Porter, G. A., Jr.; Booth, C. J.; Mehal, W. Z.; Inayat, I.; Flavell, R. A. Caspases 3 and 7: Key Mediators of Mitochondrial Events of Apoptosis. *Science* **2006**, *311*, 847−851.

(42) Danial, N. N.; Korsmeyer, S. J. Cell Death: Critical Control Points. *Cell* **2004**, *116*, 205−219.

(43) Chipuk, J. E.; Green, D. R. Do Inducers of Apoptosis Trigger Caspase-Independent Cell Death? *Nat. Rev. Mol. Cell Biol.* **2005**, *6*, 268−275.

(44) Kruman, I.; Guo, Q.; Mattson, M. P. Calcium and Reactive Oxygen Species Mediate Staurosporine-Induced Mitochondrial Dysfunction and Apoptosis in PC12 Cells. *J. Neurosci. Res.* **1998**, *51*, 293−308.

(45) Murphy, M. P. How Mitochondria Produce Reactive Oxygen Species. *Biochem. J.* **2009**, *417*, 1−13.